

A review of the lunar laser ranging technique and contribution of timing systems

AUTHORS:

Cilence Munghemzulu^{1,2}
Ludwig Combrinck^{1,2}
Joel O. Botai³

AFFILIATIONS:

¹Centre for Geoinformation Science, Department of Geography, Geoinformatics and Meteorology, University of Pretoria, Pretoria, South Africa
²Space Geodesy Programme, Hartebeesthoek Radio Astronomy Observatory, Krugersdorp, South Africa
³South African Weather Service, Pretoria, South Africa

CORRESPONDENCE TO:

Cilence Munghemzulu

EMAIL:

cilence.munghemzulu@up.ac.za

POSTAL ADDRESS:

Centre for Geoinformation Science, Department of Geography, Geoinformatics and Meteorology, University of Pretoria, Private Bag X20, Hatfield 0028, South Africa

DATES:

Received: 17 Oct. 2015
Revised: 03 Dec. 2015
Accepted: 04 Dec. 2015

KEYWORDS:

space geodetic techniques;
LLR; earth–moon system;
retroreflectors

HOW TO CITE:

Munghemzulu C, Combrinck L, Botai JO. A review of the lunar laser ranging technique and contribution of timing systems. *S Afr J Sci.* 2016;112(3/4), Art. #2015-0400, 9 pages. <http://dx.doi.org/10.17159/sajs.2016/20150400>

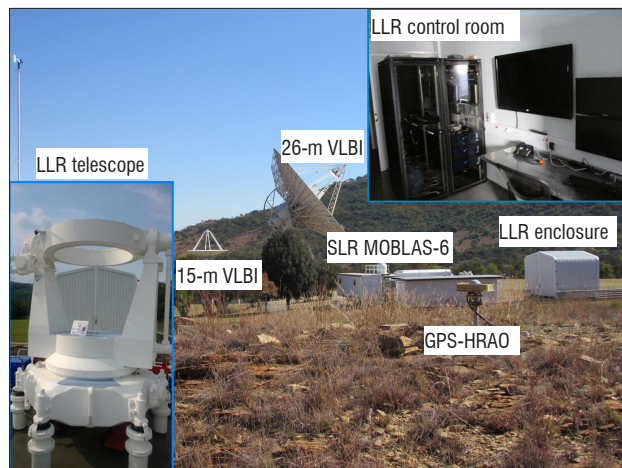
The lunar laser ranging (LLR) technique is based on the two-way time-of-flight of laser pulses from an earth station to the retroreflectors that are located on the surface of the moon. We discuss the ranging technique and contribution of the timing systems and its significance in light of the new LLR station currently under development by the Hartebeesthoek Radio Astronomy Observatory (HartRAO). Firstly, developing the LLR station at HartRAO is an initiative that will improve the current geometrical network of the LLR stations which are presently concentrated in the northern hemisphere. Secondly, data products derived from the LLR experiments – such as accurate lunar orbit, tests of the general relativity theory, earth–moon dynamics, interior structure of the moon, reference frames, and station position and velocities – are important in better understanding the earth–moon system. We highlight factors affecting the measured range such as the effect of earth tides on station position and delays induced by timing systems, as these must be taken into account during the development of the LLR analysis software. HartRAO is collocated with other fundamental space geodetic techniques which makes it a true fiducial geodetic site in the southern hemisphere and a central point for further development of space-based techniques in Africa. Furthermore, the new LLR will complement the existing techniques by providing new niche areas of research both in Africa and internationally.

Introduction

The study of earth's gravity, earth's rotation, geokinematics and inclusion of space-time currently completes the definition of space geodesy.¹ This definition has evolved from the early days of F.R. Helmert, who firstly defined geodesy as the science of the measurement and mapping of the earth's surface.^{2,3} It is clear that geodesy as a discipline has two objectives that are closely related: (1) scientific objectives constitute the study of geodynamic phenomena, the gravity field of the earth and other planets, the shape and size of the earth and its orientation in space through earth orientation parameters and (2) practical objectives include cadastral surveying to determine points accurately (up to millimetre level) on the earth's surface, accurate timing, terrestrial geodetic reference frames, and accurate positioning for civil engineering applications.² These objectives are realised through space-based techniques: Global Navigation Satellite Systems (GNSS), very long baseline interferometry (VLBI), satellite laser ranging (SLR), lunar laser ranging (LLR) and Doppler Orbitography and Radiopositioning Integrated by Satellite (DORIS). Together these techniques are fundamental in defining and maintaining different reference systems and reference frames, and determining three-dimensional station positions, velocities, earth orientation parameters and polar motion with high accuracy, spatial resolution and temporal stability.^{4,5}

The accuracy of geodetic products depends on a number of factors such as instrumental accuracies, analysis strategies, accuracy of the models used during data processing (e.g. atmospheric models), third-body perturbation effects and relativistic effects. Among these factors, the stability of timing systems plays a crucial role in determining the accuracy of the measurements. Development of highly stable clocks such as the hydrogen microwave amplification by stimulated emission of radiation (maser) and caesium clocks allows accurate timing and data correlation to be carried out with high levels of accuracy.⁶ The application of GNSS in metrology (i.e. time transfer techniques) has advanced the traditional time-keeping services (e.g. mobile reference clocks, terrestrial communication systems using Loran-C or direct radio broadcasts) and allowed comparison of clocks that are distributed around the world with high accuracy and the maintenance of Coordinated Universal Time (UTC).⁷ These timing systems contribute towards earth and space observational techniques in ensuring accurate measurements.

Earth observation and space development technologies are very important for the development of a country and have socio-economic benefits such as climatology, land management and monitoring applications. South Africa, Nigeria, Egypt, Algeria, Kenya and, more recently, Ethiopia are African countries that are harnessing space-related technologies ranging from earth observation satellites and space geodesy to radio and optical astronomy.^{8,9} The Hartebeesthoek Radio Astronomy Observatory (HartRAO) is located north of Krugersdorp in South Africa (Figure 1). It is collocated with DORIS, GNSS, 26-m and 15-m VLBI telescopes, and an SLR (MOBLAS-6) station. Currently, HartRAO is building a VGOS (VLBI2010) telescope and a new LLR system based on a 1-m aperture telescope donated by the Observatoire de la Côte d'Azur in France.¹⁰ The observatory is a fundamental (fiducial) site in the southern hemisphere as it limits geometrical errors during computation of geodetic or astronomical parameters in the global network and provides high-quality scientific data with high temporal resolution.¹⁰ Here we provide a review of the LLR technique and the importance of timing systems in light of the current development of the new LLR station at HartRAO.



VLBI, very long baseline interferometry; SLR, satellite laser ranging

Figure 1: Geodetic instruments collocated at HartRAO, South Africa. The lunar laser ranging (LLR) azimuth-elevation mount is portrayed in the inset on the left; the tube and other components were removed for upgrade and maintenance. The top right inset depicts the inside of the LLR control room.

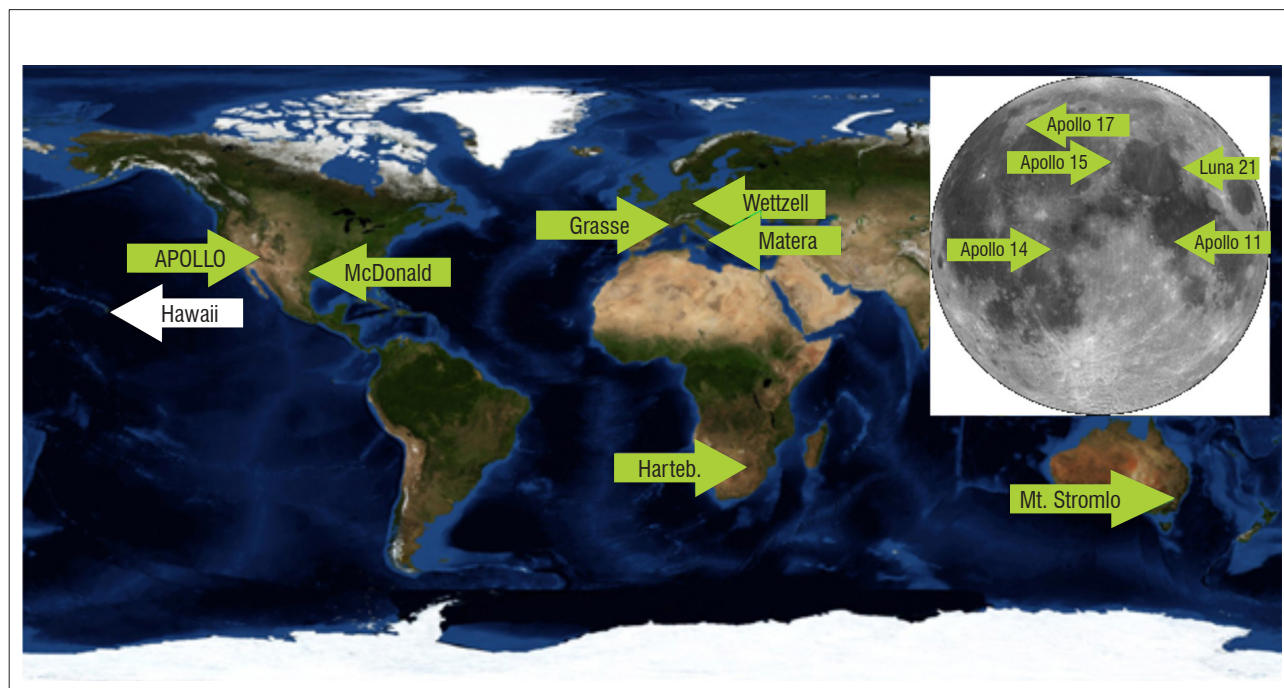
Historical developments of lunar laser ranging

The US Apollo and the Soviet missions deployed arrays of corner-cube retroreflectors on the surface of the moon during the late 1960s and 1970s; the LLR technique has therefore been used to study the earth–moon system since 1969. Currently on the moon, there are Apollo 11, 14 and 15 reflectors deployed by the Apollo missions and Lunokhod I and II reflectors deployed by the Soviet Union¹¹ (Figure 2). The McDonald Observatory was the first observatory to range to a retroreflector on the moon using a 2.7-m telescope.¹²

Currently there are four LLR stations in the world that range to the moon’s retroreflectors on a regular basis. These active stations are (1) the Apache Point Observatory Lunar Laser-ranging Operation (APOLLO), New Mexico, USA; (2) McDonald Laser Ranging Station (MLRS), Texas, USA; (3) the Observatoire de la Côte d’Azur (OCA), France; and (4) Matera, Italy.¹³ These stations are located in the northern hemisphere, which results in a weak geometry for the LLR network, as no stations are active in the southern hemisphere. However, the South African radio astronomy observatory (HartRAO), Mount Stromlo SLR observatory in Australia¹⁴, ESO La Silla Observatory IV in Chile¹⁵, National Astronomical Observatory of Japan¹⁶ and the Russians¹⁷ are planning and developing LLR stations. These additional stations will improve and contribute to the current network of the International Laser Ranging Service (ILRS) and to lunar and earth sciences as a whole.

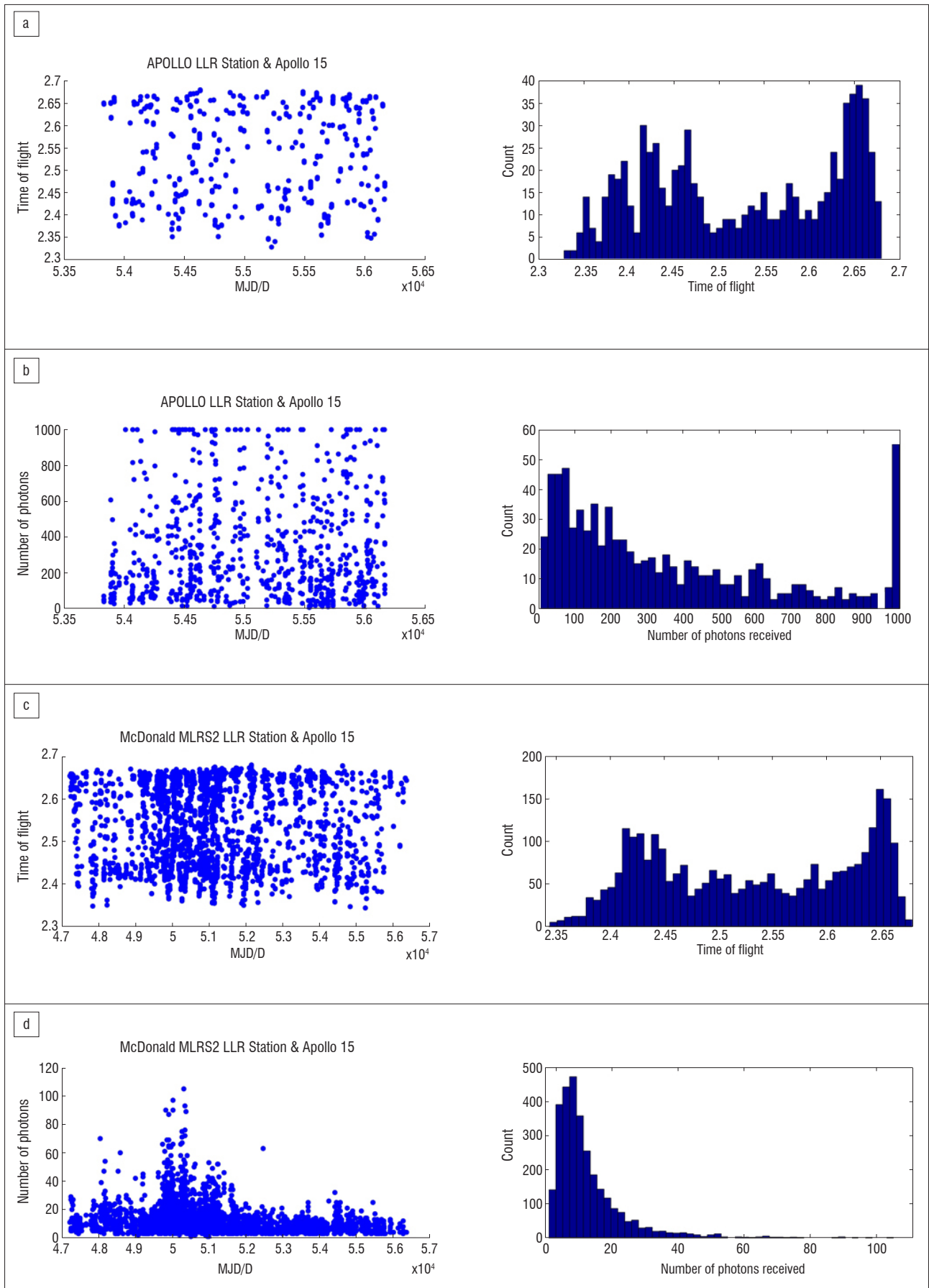
Since the LLR technique was developed, range precision has increased from about 100–250 mm to less than 20 mm.¹⁹ A similar increase in the range precision of the normal points in SLR applications has been reported in Botai et al.²⁰ and this increase has been attributed to improvements of the internal system components as well as advanced models. System component improvements can be summarised as: (1) replacement of the ruby laser with a Nd:YAG laser, (2) higher emission frequency rates (5–20 Hz), (3) faster and more sensitive detectors and (4) improved timing systems (<20 ns) with lower jitter (<10 ps) resolutions.

The existing LLR stations have provided valuable data to date. In particular, the APOLLO LLR station seems to be the only station that is capable of receiving up to 1000 photons per session (one session typically lasts for 1 h with an expected 2–10 return photons per pulse).²¹ In comparison, the photon return rates of the McDonald MLRS2 and Grasse stations range from 1 to 105 per session and from 2 to 605 per session, respectively, when ranging to the Apollo 15 retroreflector on the moon (Figure 3). The data used were provided by the Paris Observatory Lunar Analysis Center (POLAC) and are available to the public (<http://polac.obspm.fr/lrdatae.html>). Furthermore, these stations indicate that the time-of-flight to the Apollo 15 retroreflector array can range from 2.3 s to 2.7 s.



Source: International Laser Ranging Service²⁰

Figure 2: Distribution of the International Laser Ranging Service network of lunar laser ranging stations. The inset map illustrates the location of the retroreflectors on the surface of the moon.



MJD/D, modified Julian day per day

Figure 3: (a,c) Time-of-flight and (b,d) received number of photons measured between the Apollo 15 retroreflector on the moon and the APOLLO and McDonald MLRS2 stations.

Basic principles of lunar laser ranging

Ranging to the moon involves transmitting short laser pulses (about 0.03 m) from the ranging station to the retroreflectors located on the surface of the moon. The two-way time-of-flight of the laser pulses is measured on the ground using highly accurate timing systems. Most SLR stations utilise neodymium-doped yttrium aluminium garnet (Nd:YAG) lasers at a 532-nm wavelength with a repetition rate ranging from 5 Hz to 2 kHz. In SLR applications, laser energies ranging from ~1 to 100 mJ are used to range to artificial satellites such as LAGEOS. Higher laser energies (100–200 mJ) and lower laser pulse frequencies (~20 Hz) as well as larger telescopes are used for LLR applications. These differences are mainly as a result of the greater distance between the moon and the earth compared with distances between satellites that are orbiting the earth.

The basic observational equation is given in Müller et al.²² as

$$d = c \frac{\tau}{2} = |r_{em} - r_{station} + r_{reflec}| + c\Delta\tau \quad \text{Equation 1}$$

In Equation 1, d is the station to reflector distance, c is the speed of light in a vacuum, τ is the time-of-flight of the laser pulse, r_{em} describes a vector connecting the geocentre and the selenocentre (centre of mass of the moon), the geocentric position of the observatory is given by $r_{station}$ and r_{reflec} presents the selenocentric position vector of the retroreflector on the moon. The laser pulse is delayed as a result of interaction with the non-linear atmospheric environment, which must be corrected for. Other factors that must be corrected for are discussed later in this paper. The term $\Delta\tau$ describes these corrections, which must be applied to obtain an accurate computed distance.

The earth–moon distance is approximately 385 000 km; unlike in SLR, this distance presents a challenge in LLR because fewer photons are received per single laser shot containing about 10^{15} photons. To illustrate the impact of the earth–moon distance on the photon return rate, Degnan²³ provided a radar link equation that estimates the success of receiving photoelectrons n_{pe} as detected by the receiving telescope as:

$$n_{pe} = \eta_q \left(E_T \frac{\lambda}{hc} \right) \eta_T G_T \sigma \left(\frac{1}{4\pi R^2} \right)^2 A_r \eta_R T_a T_c^2, \quad \text{Equation 2}$$

where η_q is the detector's quantum efficiency, E_T is the laser pulse energy, λ is the wavelength of the laser, h is Planck's constant, c is the speed of light in a vacuum, η_T is the efficiency of the transmitter optics, G_T is the transmitter gain, σ is the reflector optical cross section and η_R is the efficiency of the receiver optics. The effective area of the telescope receiving aperture is given by A_r , T_a is the one-way atmospheric transmission if present, and T_c is the one-way transmissivity of cirrus cloud. R is the slant range to the moon and can be calculated using:

$$R = -(R_E + h_s) \cos \theta_{zen} + \sqrt{(R_E + h_s)^2 \cos^2 \theta_{zen} + 2R_E (h_s - h_t) + h_s^2 - h_t^2}, \quad \text{Equation 3}$$

where R_E is earth's radius (6378 km), h_t is the station height above sea level, h_s is the moon altitude above sea level, and θ_{zen} is the zenith angle of the moon as observed from the ranging station.

The observed raw data (d_{oi}) are filtered to detect gross errors, evaluated to access the accuracy of the observations and compressed for further analysis in the form of a normal point (NP) data set (Equation 4).²³ The residuals are computed from the predicted and observed ranges and the outliers are removed using a range window. A suitable trend function (a polynomial fit or a set of orbital parameters) is usually fitted to the residuals to detect further outliers by analysing the deviations from the fit (\bar{f}_i). The data can then be divided into bins; there is a recommended number of bins to be used for different retroreflectors/satellites, e.g. for LAGEOS 1 and 2, a 120-s bin width is used to divide the data for the duration of the observation. For each bin interval, i , a mean value (\bar{f}_i) of all deviations is calculated and added to the trend function at the centre of the interval.²³ This point is referred to as a normal point and thus represents a single observation of the particular interval,

$$NP_i = d_{oi} - (f_i - \bar{f}_i). \quad \text{Equation 4}$$

The systematic errors, some of which are discussed later, must still be modelled out during further processing. The internal system accuracy of the station (i.e. the root mean square, RMS) can be evaluated using Equation 5 as given in Sinclair²⁴, where n_i represents the number of observations within the bin.

$$RMS_i = \sqrt{\frac{1}{n_i} \sum_j (f_{ij} - \bar{f}_i)^2}. \quad \text{Equation 5}$$

Timing systems and current progress on the new LLR station

Earth was once thought to function as a perfect clock by counting the number of sunrises or sunsets and constructing a calendar as earth rotates around its axis. Advancements have been made in the more accurate measurement of time and short intervals through the development of mechanical clocks; pendulum clocks were built with an accuracy of about 10 s per day.²⁵ However, it is important to note that during this period there was no method to synchronise individual clocks.

The development of timing systems has also led to the development of many technologies that are of societal benefit and that we take for granted, such as GPS, the electric power grid and mobile phones.²⁶ The reported accuracy of the first operational atomic clock was 0.1 ms/day.²⁷ Accuracy of caesium atomic clocks increased with the development of laser cooling technologies; the National Institute of Standards and Technology (NIST) has so far developed NIST-F1 and NIST-F2, which have an accuracy of more than 10^{-15} at 1 s – the most accurate caesium clocks to date.²⁸ Quartz and rubidium clocks are used in scientific applications such as LLR and SLR as they are relatively affordable and also offer a high accuracy of about 10^{-12} at 1 s.

HartRAO currently is developing a LLR station by utilising a 1-m aperture Cassegrain telescope donated by the French Observatoire de la Côte d'Azur.²⁹ The LLR station is designed to range to retroreflectors mounted on satellites and the surface of the moon. The LLR station will use a newly developed 4393A rubidium timing reference system by Microsemi with an accuracy to sub-picosecond ($<10^{-12}$) level. This system will improve the measurement of time-of-flight of the laser pulses and limit instrumentation error dependency. Detailed current development and future perspectives of the LLR system are described in Combrinck¹⁰.

Factors contributing to range bias

In light of the new LLR analysis software being developed at HartRAO, it is necessary to take into account all the factors that affect ranging to the moon and satellites, and which eventually affect the accuracy of determining the moon's orbit. In terms of SLR, these factors are listed in Combrinck and Suberlak³⁰ and Combrinck³¹ as: earth's geopotential³², solid earth tides³³, ocean tides, planetary third-body perturbation (sun, moon and planets), relativistic acceleration³⁴, atmospheric tide and atmospheric drag³⁵, solar radiation pressure³⁶, earth radiation pressure, thermal radiation acceleration³⁷, lunar librations³⁸ (for LLR), Shapiro delay³⁹, tropospheric delay⁴⁰ and delay induced by electronic systems. Two separate software suites will be used for either SLR or LLR analysis, because although some of the corrections are similar (e.g. station displacement due to solid earth tides), the analysis problem is quite different. Not all of these factors are discussed here; further information can be found in the references provided. Corrections for a few factors are applied to illustrate the importance of considering these factors in the LLR analysis package. In a simplified version, the time-of-flight of the laser pulses can be described by

$$ToF = T_{sy} + D_{at} + G_{rt} + T_{td} + \epsilon \quad \text{Equation 6}$$

where T_{sy} represents actual time interval measurement by the station, D_{at} is the time delay due to the atmosphere, G_{rt} is the general relativity correction, T_{td} is the time variation induced by tidal effects and ϵ includes all other corrections not listed above and unknowns. Time-of-flight

is the actual time interval measurement at the station and comprises several components. The station timing system measures the gross sum of contributions as a time interval. T_{sy} is the 'true' satellite distance (expressed as time-of-flight). Data processing is applied mainly to account for the true satellite distance by removing the other disturbing contributions. Practical examples are given below for selected parameters to illustrate their importance.

Tidal correction on station position

The gravitational attractions on earth of the sun, moon and planets, result in a force that deforms the earth's gravitational field and induces solid earth tides.⁴¹ This force is coupled with ocean and atmospheric loading effects as well as the mantle convection processes within the earth. The earth system responds to these effects through mass displacement, rotational acceleration and continuous deformation of the solid crust.³⁰ Space geodetic instruments such as LLR are affected by these continuous deformation effects, which translate to an additional range bias during ranging. Hence, the LLR analysis software (currently under development at HartRAO) must be able to model these effects with high accuracy in order to improve the range bias. The earth tide, pole tide and ocean tide effects are well described in McCarthy and Petit⁴² and readers are referred to this reference for more information.

The solid earth tides can be conveniently modelled⁴³ as variations in the standard geopotential coefficients C_{nm} and S_{nm} , and can be described as

$$\Delta\bar{C}_{nm} - i\Delta\bar{S}_{nm} = \frac{k_{nm}}{2n-1} \sum_{j=2}^3 \frac{GM_j}{GM_E} \left(\frac{R_e}{r_j}\right)^{n+1} \bar{P}_{nm}(\sin\Phi_j) e^{-im\lambda_j} \{with \bar{S}_{n0}=0\}$$

Equation 7

where k_{nm} is the nominal Love number for degree n and order m , R_e represents the equatorial radius of the earth, GM_E is the gravitational parameter for the earth; the gravitational parameter for the moon ($j=2$) and sun ($j=3$) is given by GM_j , the distance to the geocentre of the moon or sun is represented by r_j , Φ_j is the body fixed geocentric latitude of the moon or sun, λ_j represents body fixed east longitude (from Greenwich) of the moon or sun and \bar{P}_{nm} represents the normalised associated Legendre function.

A library developed in Fortran to compute station displacement due to earth tides was developed by Petrov³³ and is currently used by the Satellite Data Analysis Software (SDAS) developed at HartRAO³⁰. The same library was also used in this study to illustrate the effects of earth tide on the earth crust for the HartRAO site, where the LLR telescope is located. A continuous station displacement can be clearly seen, with magnitudes ranging from -160 mm to 300 mm in vertical displacement (Figure 4).

Gravitational pull by the sun, moon and planets also results in ocean tides; an additional weight by ocean loading influences crustal displacement and results in temporal variations of station position. Stations that are inland are expected to be less affected than those that are close to the coast. There are plans to move the new LLR station at HartRAO, once completed, to Matjiesfontein in the Great Karoo (in the Western Cape of South Africa).²⁹ This new site is about 240 km from the Southern Ocean; the effect of ocean tides is expected to be greater at the new site than at the current location (HartRAO, Krugersdorp). In order to better understand and model the effects of ocean and earth tides, atmospheric loading and local hydrological cycles, instruments such as a superconducting gravimeter are required, and should be mounted as close as possible to the ranging telescope to measure small displacements. A typical example is the APOLLO station at Apache Point, Texas: their gravimeter has a noise level of 1 nm/s², which is very sensitive and can model these effects to millimetre accuracy or better.²¹ HartRAO has installed a gravimeter to compensate for these effects and improve the existing models.

Tropospheric delay correction

The troposphere introduces a significant delay (up to several metres) both in radio and optical wavelengths. Different models have been developed to account for this delay in optical wavelength observations⁴⁴ and radio wavelength observations⁴⁰. The delay increases with decreasing elevation angles. Usually, observations are made at higher elevation angles (e.g. above 20° for SLR or LLR). Data from a network of radiosonde distributed worldwide are used to create and validate tropospheric models. A series of mapping functions is used to account for tropospheric delay in the form of⁴⁰:

$$\Delta L(\epsilon) = \Delta L_h^z \cdot mf_h(\epsilon) + \Delta L_w^z \cdot mf_w(\epsilon),$$

Equation 8

where the total slant delay ΔL as a function of an elevation angle ϵ is expressed as the sum of a hydrostatic and a wet portion – both can be expressed as the product of a zenith delay and a corresponding mapping function. To illustrate the extent of the delay introduced by the troposphere at different elevation angles for radio frequencies, we used the GPT2w model developed by Böhm et al.⁴⁰ to estimate slant delay for the HartRAO site. Figure 5 depicts computed slant delay correction at different elevations. An example of the delay in optical wavelength (532 nm) for a 7-day arc of several SLR stations is given in Combrinck³¹, based on the model developed by Mendes and Pavlis⁴⁴. It must be noted that the delay in radio and optical wavelengths is different but the pattern is the same (i.e. the delay increases with a decrease in elevation angle). For the purpose of LLR analysis software, appropriate models will be implemented to compensate for atmospheric effects.

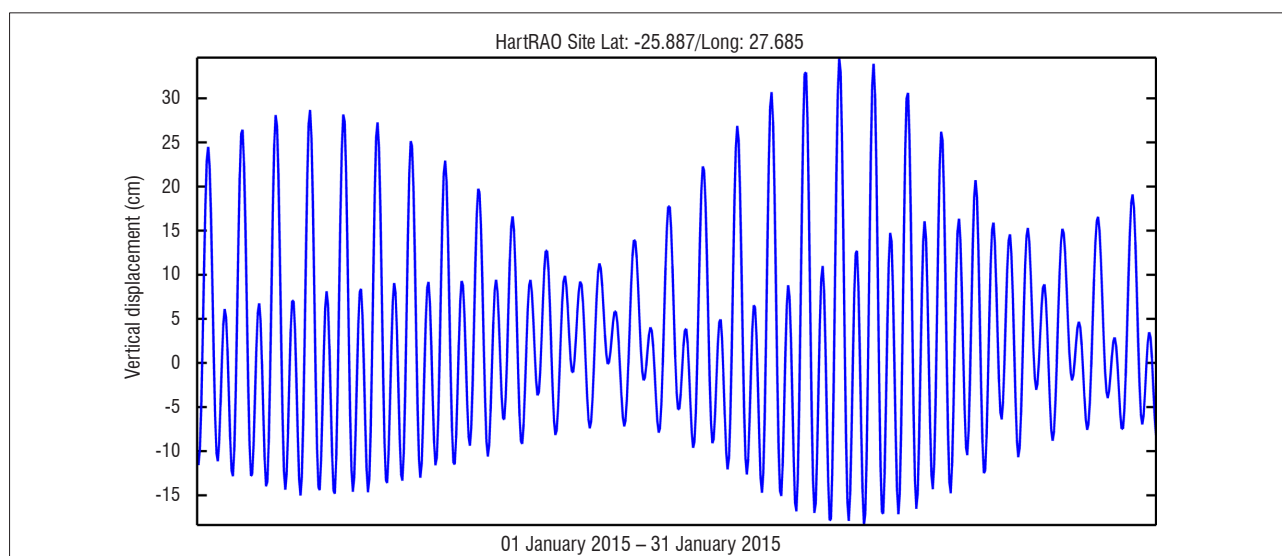


Figure 4: Station vertical displacement for the HartRAO site, simulated for the month of January 2015.

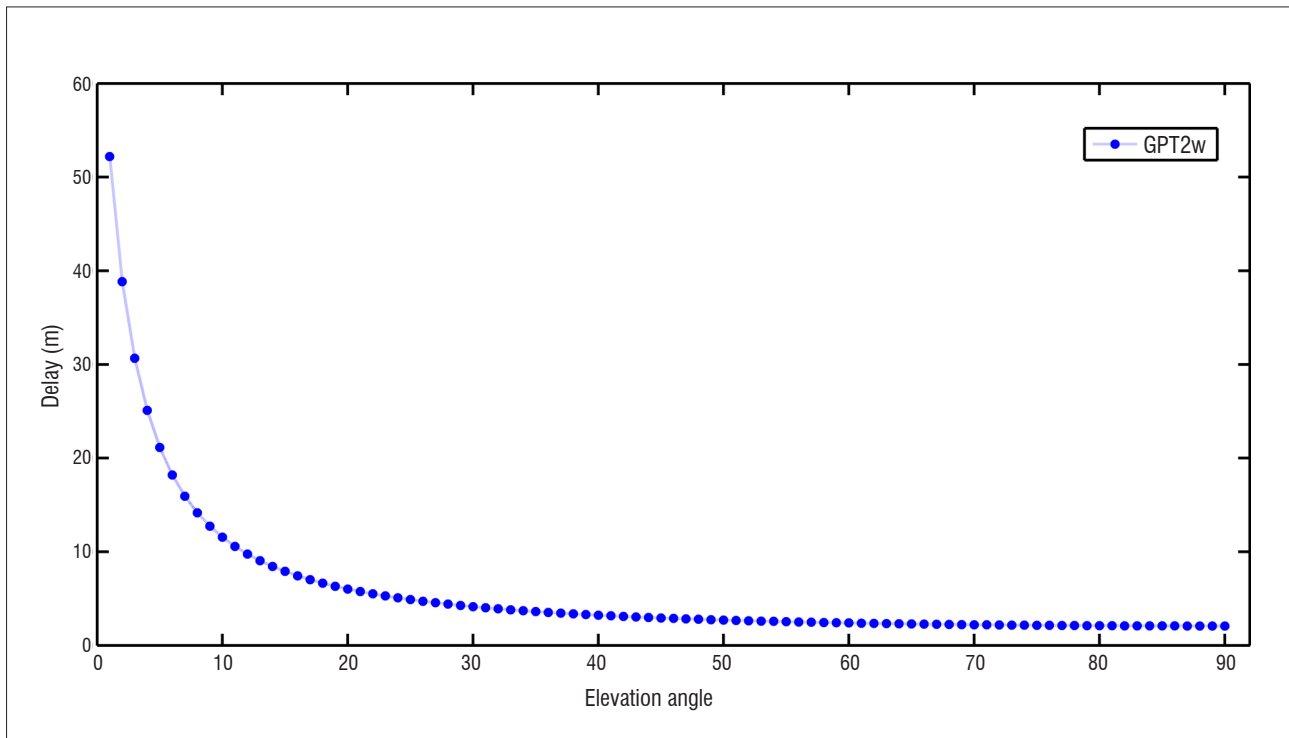


Figure 5: Slant delay as a function of elevation angle for the HartRAO site, computed for the day of 30 June 2015, using Böhm et al.'s⁴⁰ GPT2w model.

Timing systems

Timing systems are crucial in space geodetic and astronomical instrumentation. In particular, the accuracy of measurements depends on the accuracy of the reference timing systems. Most reference timing stations for SLR and LLR are at the level of 10^{-12} Allan deviation at 1 s using rubidium/quartz crystal oscillators⁴⁵, while the hydrogen maser clocks used in VLBI techniques are better than 10^{-14} at 1 s.⁴⁶ Most stations are limited in their use of highly accurate timing systems such as maser clocks because of their high cost. The noise levels within event timers and photon detection systems also play a crucial role in the accuracy of the normal data points and range bias. It is envisaged that the new LLR station will use the newly developed 4380A-GPS disciplined master timing reference by Microsemi Corporation. This unit has an Allan deviation of 10^{-13} at 1 s and less than 10 ns RMS timing accuracy. A low jitter event timer of 3 ps RMS and a solid state photon detector (a single-photon avalanche diode or SPAD) with a quantum efficiency of 50% will be integrated to allow for sub-centimetre ranging precision.

An impact of timing systems on the observed range measurements can be clearly seen from Figure 6, in which a normal point data quality of the Potsdam SLR station between 2003 and 2011 indicates high variation, ranging from 10 mm to 25 mm.⁴⁵ During 2011, an old timing system was replaced with a more modern timing system with better specifications (Table 1). The SPAD with a quantum efficiency of 28% was replaced with a SPAD with a quantum efficiency of 40% and low jitter. As a result, the normal point data are characterised by low variations, which can be directly linked to the improvement of the timing systems (among others) post 2011.

Lunar laser ranging contributions to science and society

Earth observation techniques have a direct impact on the social lives of people. Imagery from remote sensing techniques is widely applied in areas such as agriculture⁴⁷, ecosystem management^{48,49}, water management⁵⁰, disaster management⁵¹ and weather applications⁵². These applications provide examples of the use of earth observation

techniques to assist in planning, early warning systems for natural disasters, and management of earth's resources. More advanced remote sensing techniques such as VLBI, GNSS, LLR and SLR contribute in the same way as satellite remote sensing does to society. The derived data products – such as the International Terrestrial Reference Frame (ITRF), the International Celestial Reference Frame, earth orientation parameters, the gravity field, and atmosphere and ionosphere parameters – form part of the foundation of earth observation technologies.⁵³ A set of station coordinates and velocities derived from the geodetic techniques is used to construct a reference frame that allows connection and comparison between different geodetic data sets over varying space and time. This construction is done through combination of the data sets using scientific software such as CATREF⁵⁴ and by taking into account the local site ties. The latest ITRF2008 has an accuracy to sub-centimetre.⁴ This system provides a basis for local reference frame systems, which are realised based on the ITRF, including, for example, the unified African Geodetic Reference Frame (AFREF), which can be used for cadastral surveys, mapping and civil engineering applications.⁵⁵

The LLR technique in particular contributes towards advancement of the field of space geodesy, lunar science, earth–moon system dynamics and gravitational physics. The increased accuracy in range measurements from 200–300 mm in early development stages to about 20–30 mm in recent developments, has provided ways to test and evaluate general relativity theory⁵⁶ and the gravitational constant with ranging accuracy at picosecond level. Williams et al.⁵⁷ derived geophysical and orbit parameters of the moon; the gravitational constant was evaluated to be $G/G = 4 \pm 9 \times 10^{-13}$ per year by Williams et al.⁵⁸ and a more recent value of $-0.7 \pm 3.8 \times 10^{-13}$ per year is reported by Hofmann et al.⁵⁹ The LLR system at HartRAO is being developed by HartRAO staff and PhD and MSc students registered at various South African universities, hence capacity building and skills transfer are at a high level. This project will support environmental monitoring through proxy parameters which measure, for example, the state of the atmosphere, gravity fields (for groundwater storage monitoring) and seismic activities, which are important to society.

Table 1: Historical improvement of the Potsdam satellite laser ranging station timing system⁴⁵

Timing equipment	Date of installation/replacement		
	20 July 2001	2001–2004	01 May 2011
Detection type	SPAD (AD230)		SPAD (MPD-ICTC)
Quantum efficiency (%)	28		40
Jitter (ps)	75		20
Signal processor	CFD (TC4S4)		
Time measurement	Interval	Event	Event
Model	SR620	A031-ET	A032-ET
Resolution (ps)	4	1	1
Precision (ps)	20	10	7

SPAD, single-photon avalanche diode; CFD, constant fraction discriminator

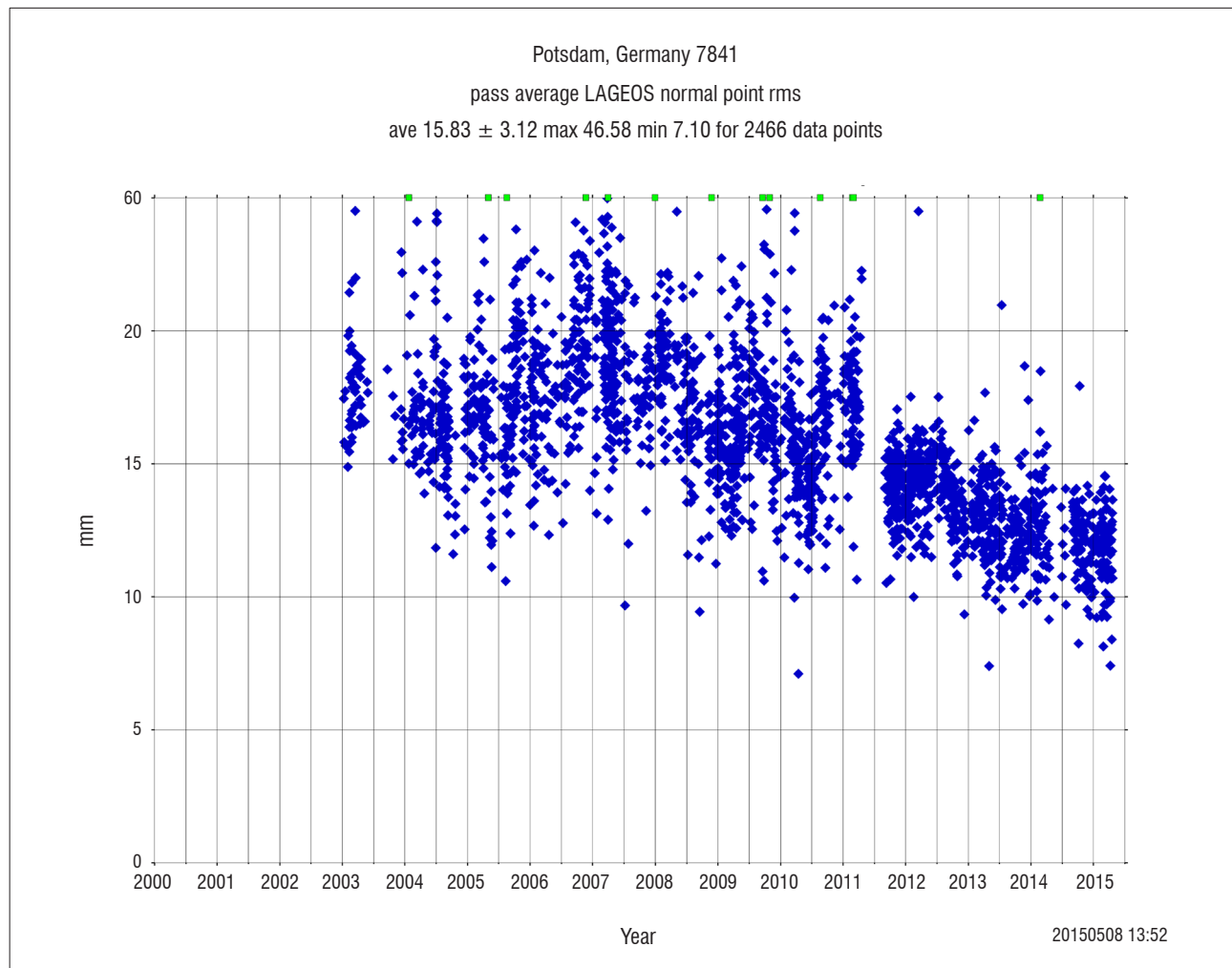


Figure 6: Potsdam satellite laser ranging station performance, measured based on normal point root mean square for LAGEOS ranging data. The single-photon avalanche diode was replaced with one of higher specifications in 2011.⁴⁵

Conclusion

We have briefly reviewed the LLR technique and the timing systems in light of the new LLR station at HartRAO. The difficulties associated with ranging to the moon were highlighted, and factors that contribute to range bias were emphasised as these must be incorporated in the LLR analysis software. This new LLR station will contribute to both local and global communities to meet the scientific objectives of the currently growing space science endeavours by many countries as well as support socio-economic developments. Existing LLR stations are sparsely distributed globally and the station at HartRAO (currently in development) together with Mount Stromlo SLR observatory in Australia have the opportunity to expand the existing global network to the southern hemisphere.

Data products derived from highly technical space geodetic techniques such as LLR have indirect and direct benefits to society, hence the LLR project at HartRAO has received local support and international support from organisations such as the National Aeronautics and Space Administration (USA) and the Observatoire de la Côte d'Azur (France). There are a number of factors that must be taken into consideration during the implementation of the LLR analysis software. The first step is to ensure that highly accurate (to sub-picosecond level) timing sub-systems are implemented to minimise local systematic errors. The delay induced by the environment can be modelled with current existing algorithms to a high level of confidence. This new LLR station will open many opportunities for current and future space programmes, with societal benefits, both in Africa and internationally.

Acknowledgements

This research was financially supported by the National Research Foundation (NRF), the Department of Science and Technology and Inkaba yeAfrica. Lunar laser ranging data were provided by the Paris Observatory Lunar Analysis Center (POLAC). Support from Observatoire de la Côte d'Azur (OCA) and NASA is also acknowledged.

Authors' contributions

C.M. conceptualised, designed and wrote the original draft manuscript; L.C. and J.O.B. modified, edited and approved the manuscript.

References

1. Combrinck L. A comparison of general relativity theory evaluations using VLBI and SLR: Will GGOS improve these results? In: Behrend D, Baver K, editors. IVS 2012 General Meeting Proceedings; 2012 March 4–9; Madrid, Spain. Greenbelt, MD: International VLBI Service for Geodesy and Astrometry; 2012. p. 357–361.
2. Torge W, Müller J. Geodesy. 4th ed. Berlin: Walter de Gruyter; 2012. p. 433. <http://dx.doi.org/10.1515/9783110250008>
3. Helmert FR. Die mathematischen und physikalischen Theorien der höheren Geodäsie [The mathematical and physical theories of higher geodesy]. Leipzig: Die mathematischen Theorien; 1880.
4. Altamimi Z, Collilieux X, Metivier L. ITRF2008: An improved solution of the international terrestrial reference frame. *J Geod*. 2011;85(5):457–473. <http://dx.doi.org/10.1007/s00190-011-0444-4>
5. Lu Z, Qu Y, Qiao S. Geodesy: Introduction to geodetic datum and geodetic systems. Berlin: Springer-Verlag; 2014. <http://dx.doi.org/10.1007/978-3-642-41245-5>
6. Wynands R, Weyers S. Atomic fountain clocks. *Metrologia*. 2005;42(3):S64. <http://dx.doi.org/10.1088/0026-1394/42/3/S08>
7. Lombardi MA. Chapter 17: Fundamentals of time and frequency. In: Bishop RH, editor. The mechatronics handbook. Boca Raton, FL: CRC Press; 2002. Available from: <http://www.sze.hu/~szenasy/Szenzorok%20%E9s%20aktu%E1torok/Szenzakt%20jegyzetek/Mechatronics%2520handbook%5B1%5D.pdf>
8. Martinez P. Space science and technology in South Africa: An overview. *African Skies/Cieux Africains*. 2008;12:46–49.
9. Ngcofe L, Gottschalk K. The growth of space science in African countries for earth observation in the 21st century. *S Afr J Sci*. 2013;109(1/2), Art. #a001, 5 pages. <http://dx.doi.org/10.1590/sajs.2013/a001>
10. Combrinck L. Development of a satellite and lunar laser ranger and its future applications. Paper presented at: The 62nd International Astronautical Congress; 2011 October 03–07; Cape Town, South Africa. Paris: International Astronautical Federation; 2011. IAC-11-A2.1. <http://dx.doi.org/10.13140/2.1.1743.3928>
11. Williams JG, Newhall XX, Dickey JO. Relativity parameters determined from lunar laser ranging. *Phys Rev D*. 1996;53(12):6730–6738. <http://dx.doi.org/10.1103/PhysRevD.53.6730>
12. Barker ES, Calame O, Mulholland JD, Shelus PJ. Improved coordinates for Lunokhod 2 based on laser observations from McDonald Observatory. *Space Res*. 1975;XV:71–74.
13. Hofmann F, Müller J, Biskupek L, Mai E, Torre JM. Lunar laser ranging – What is it good for? Paper presented at: The 18th International Workshop on Laser Ranging; 2013 November 11–15; Fujiyoshida, Japan. Available from: <http://cddis.gsfc.nasa.gov/lw18/docs/papers/Session9/13-04-02-MuellerJM.pdf>
14. Greene B, McK Luck J. LLR developments at Mount Stromlo. Paper presented at: The 13th International Workshop on Laser Ranging; 2002 October 07–11; Washington DC, USA. Available from: http://cddis.gsfc.nasa.gov/lw13/docs/papers/llr_greene_1m.pdf
15. Fienga A, Courde C, Torre JM, Manche H, Murphy T, Mueller J, et al. Interests of a new lunar laser instrumentation on the ESO NTT telescope [arXiv:1405.0473 astro-ph.IM]. c2014 [cited 2015 Jun 15]. Available from: <http://arxiv.org/abs/1405.0473>
16. Noda H, Kunimori H, Araki H. Lunar laser ranging experiment at Koganei SLR station. Presented at: The 45th Lunar and Planetary Science Conference; 2014 March 17–21; The Woodlands, TX, USA. Available from: <http://www.hou.usra.edu/meetings/lpsc2014/pdf/1638.pdf>
17. Vasilyev MV, Yagudina EI, Torre J-M, Feraudy D. Planned LLR station in Russia and its impact on the lunar ephemeris accuracy [article on the Internet]. c2014 [cited 2015 Sep 01]. Available from: <http://syrite.obspm.fr/jsr/journees2014/pdf/Vasilyev.pdf>
18. International Laser Ranging Services (ILRS). LLR map of stations [image on the Internet]. c2009 [updated 2015 Feb 04; cited 2015 May 17]. Available from: <http://ilrs.gsfc.nasa.gov/science/scienceContributions/lunar.html>
19. Murphy T. Lunar laser ranging: A laboratory for gravity. Proceedings of SLAC Conferences, Workshops & Symposia, 2007/08/09 [document on the Internet]. c2007 [cited 2015 Jun 30]. Available from: <http://www-conf.slac.stanford.edu>
20. Botai CM, Combrinck L, Botai JO. Satellite laser ranging measurements in South Africa: Contributions to earth system science. *S Afr J Sci*. 2015;111(3/4), Art. #2013-0193, 9 pages. <http://dx.doi.org/10.17159/sajs.2015/20130193>
21. Murphy T, Adelberger E, Battat J, Colmenares N, Crossley D, Holye CD, et al. APOLLO performance and data quality. Paper presented at: The 19th International Workshop on Laser Ranging; 2014 October 27–31; Annapolis, MD, USA. Available from: http://cddis.gsfc.nasa.gov/lw19/docs/2014/Papers/3061_Murphy_paper.pdf
22. Müller J, Williams JG, Turyshev SG. Lunar laser ranging contributions to relativity and geodesy. In: Dittus H, Lammerzahl C, Turyshev SG, editors. Laser, clocks and drag-free control: Exploration of relativistic gravity in space. Berlin: Springer; 2008. p. 457–472. http://dx.doi.org/10.1007/978-3-540-34377-6_21
23. Degnan J. Millimetre accuracy satellite laser ranging. In: Smith DE, Turcotte DL, editors. Contributions of space geodesy to geodynamics: Crustal dynamics. Geodynamics Series 25. Washington DC: American Geophysical Union; 1993. p. 133–162.
24. Sinclair AT. Data screening and normal point formation: Re-Statement of Herstmonceux Normal Point Recommendation [homepage on the Internet]. c1997 [updated 2015 Feb 04; cited 2015 May 17]. Available from: http://ilrs.gsfc.nasa.gov/data_and_products/data/npt/npt_algorithm.html
25. Lombardi MA. The evolution of time measurement part 2: Quartz clocks. *IEEE Instrumentation & Measurement Magazine*. 2011;14(5):41–48.

26. Lombardi MA. The evolution of time measurement part 3: Atomic clocks. *IEEE Instrumentation & Measurement Magazine*. 2011;14(6):46–49. <http://dx.doi.org/10.1109/MIM.2011.6086901>
27. Henderson D. Essen and the National Physical Laboratory's atomic clock. *Metrologia*. 2005;42(3):S4. <http://dx.doi.org/10.1088/0026-1394/42/3/S02>
28. Heavner TP, Donley EA, Levi F, Costanzo G, Parker TE, Shirley JH, et al. First accuracy evaluation of NIST-F2. *Metrologia*. 2014;51(3):174–184. <http://dx.doi.org/10.1088/0026-1394/51/3/174>
29. Combrinck L, Botha R. Challenges and progress with the development of a lunar laser ranger for South Africa. Paper presented at: The 18th International Workshop on Laser Ranging; 2013 November 11–15; Fujiyoshida, Japan. Available from: <http://cdiss.gsfc.nasa.gov/lw18/docs/papers/Session13/13-05-04-Combrinck.pdf>
30. Combrinck L, Suberlak V. Earth-tide as parameter of crustal motion correction for SLR station displacement. *S Afr J Geol*. 2007;110(2–3):203–210. <http://dx.doi.org/10.2113/gssajg.110.2-3.203>
31. Combrinck L. Satellite laser ranging. In: Xu G, editor. *Sciences of geodesy I: Advances and future directions*. Berlin: Springer-Verlag; 2010. p. 302–336. http://dx.doi.org/10.1007/978-3-642-11741-1_9
32. Botai MC, Combrinck L. Investigating the accuracy of gravity field models using satellite laser ranging data. *S Afr J Geol*. 2011;114(3–4):539–544. <http://dx.doi.org/10.2113/gssajg.114.3-4.535>
33. Petrov L. Software sotid for computation of site displacements due to the solid earth tides: Updated pdf documentation 2005.02.11 [document on the Internet]. c2005 [cited 2015 Jun 30]. Available from: <http://gemini.gsfc.nasa.gov/sotid>
34. Combrinck L. General relativity and space geodesy. In: Xu G, editor. *Sciences of geodesy II: Innovation and future developments*. Berlin: Springer-Verlag; 2013. p. 53–95. http://dx.doi.org/10.1007/978-3-642-28000-9_2
35. Van Dam TM, Herring TA. Detection of atmospheric pressure loading using very long baseline interferometry measurements. *J Geophys Res*. 1994;99(B3):4505–4517. <http://dx.doi.org/10.1029/93JB02758>
36. Ziebart M. High precision analytical solar radiation pressure modelling for GNSS spacecraft [PhD thesis]. London: University of East London; 2001.
37. Vokrouhlický D. A note on the solar radiation perturbations of lunar motion. *Icarus*. 1997;126(2):293–300. <http://dx.doi.org/10.1006/icar.1996.5652>
38. Mulholland JD, Silverberg EC. Measurement of physical librations using laser retroreflectors. *Moon*. 1972;4(1–2):155–159. <http://dx.doi.org/10.1007/BF00562923>
39. Shapiro LI. Fourth test of general relativity. *Phys Rev Lett*. 1964;13:789–791. <http://dx.doi.org/10.1103/PhysRevLett.13.789>
40. Böhm J, Möller G, Schindelegger M, Pain G, Weber R. Development of an improved empirical model for slant delays in the troposphere (GPT2w). *GPS Solutions*. 2015;19(3):433–441. <http://dx.doi.org/10.1007/s10291-014-0403-7>
41. Métivier L, Viron O, Conrad CP, Renault S, Diament M, Patau G. Evidence of earthquake triggering by the solid earth tides. *Earth Planet Sci Lett*. 2009;278(3–4):370–375. <http://dx.doi.org/10.1016/j.epsl.2008.12.024>
42. McCarthy D, Petit G, editors. *IERS conventions (2003)*. IERS Technical Note 32. Frankfurt: Verlag des Bundesamts für Kartographie und Geodäsie; 2004. Available from: http://www.iers.org/SharedDocs/Publicationen/EN/IERS/Publications/tn/TechnNote32/tn32.pdf?__blob=publicationFile
43. Eanes RJ, Schutz B, Tapley B. Earth and ocean tide effects on Lageos and Starlette. In: Kuo JT, editor. *Proceedings of the Ninth International Symposium on Earth Tides*. Stuttgart: Sckweizerbart'sche Verlagabuchhandlung; 1983. p. 239–249.
44. Mendes VB, Pavlis EC. High-accuracy zenith delay prediction at optical wavelengths. *Geophys Res Lett*. 2004;31(14):L14602. <http://dx.doi.org/10.1029/2004GL020308>
45. International Laser Ranging Services (ILRS). LLR station log files [image on the Internet]. c2009 [updated 2015 Feb 04; cited 2015 Jun 30]. Available from: <http://ilrs.gsfc.nasa.gov/network/stations/index.html>
46. International VLBI Service for Geodesy and Astrometry. Station log files [homepage on the Internet]. c2015 [updated 2015 Jun 30; cited 2015 Jun 30]. Available from: <http://ivscc.gsfc.nasa.gov/about/org/components/ns-list.html>
47. Bastiaanssen WGM, Molden DJ, Makin LW. Remote sensing for irrigated agriculture: Examples from research and possible applications. *Agr Water Manage*. 2000;46(2):137–155. [http://dx.doi.org/10.1016/S0378-3774\(00\)00080-9](http://dx.doi.org/10.1016/S0378-3774(00)00080-9)
48. Kerr TJ, Ostrovsky M. From space to species: Ecological applications for remote sensing. *Trends Ecol Evol*. 2003;18(6):299–305. [http://dx.doi.org/10.1016/S0169-5347\(03\)00071-5](http://dx.doi.org/10.1016/S0169-5347(03)00071-5)
49. Cohen WB, Goward SN. Landsat's role in ecological applications of remote sensing. *BioScience*. 2004;54(6):535–545. [http://dx.doi.org/10.1641/0006-3568\(2004\)054\[0535:LRIEAO\]2.0.CO;2](http://dx.doi.org/10.1641/0006-3568(2004)054[0535:LRIEAO]2.0.CO;2)
50. Jackson TJ, Schmutge J, Engman ET. Remote sensing applications to hydrology: Soil moisture. *Hydrolog Sci J*. 1996;41(4):517–530. <http://dx.doi.org/10.1080/02626669609491523>
51. Madry S. *Space systems for disaster warning, response, and recovery*. New York: Springer; 2015. <http://dx.doi.org/10.1007/978-1-4939-1513-2>
52. Lazzara MA, Coletti A, Diedrich BJ. The possibilities of polar meteorology, environmental remote sensing, communications and space weather applications from Artificial Lagrange Orbit. *Adv Space Res*. 2011;48(11):1880–1889. <http://dx.doi.org/10.1016/j.asr.2011.04.026>
53. Rothacher M. Towards a rigorous combination of space-geodetic techniques. In: Richter B, Schwegmann W, Dick WR, editors. *Proceedings of the IERS Workshop on Combination Research and Global Geophysical Fluids; 2002 November 18–21; Munich, Germany*. Frankfurt: Verlag des Bundesamts für Kartographie und Geodäsie; 2003. p. 7–18.
54. Altamimi Z, Sillard P, Boucher C. CATREF software: Combination and analysis of terrestrial reference frames. Technical manual [document on the Internet]. c2006 [cited 2015 Jul 02]. Available from: <http://grgs.obs-mip.fr/en/content/download/303/2351/file/CATREF-1.pdf>
55. Drewes H, Hornik H. *Travaux volume 38: Reports 2011–2013*. Munich: International Association of Geodesy; 2013. Available from: http://iag.dgfi.tum.de/fileadmin/IAG-docs/Travaux_2011-2013.pdf
56. Müller J, Williams J, Turyshev S, Shelus P. Potential capabilities of lunar laser ranging for geodesy and relativity. In: Tregoning P, Rizos C, editors. *Dynamic planet. IAG Symposia volume 130*. Berlin: Springer; 2007. p. 903–909. http://dx.doi.org/10.1007/978-3-540-49350-1_126
57. Williams JG, Boggs DH, Folkner WM. DE421 lunar orbit, physical librations, and surface coordinates [Interoffice memorandum JPL IOM 335-JW, DB, WF-20080314-001]. 2008 March 14. Available from: ftp://ssd.jpl.nasa.gov/pub/eph/planets/ioms/de421_moon_coord_iom.pdf
58. Williams JG, Turyshev SG, Boggs DH. Progress in lunar laser ranging tests of relativistic gravity. *Phys Rev Lett*. 2004;93(26), Art. #261101, 4 pages. <http://dx.doi.org/10.1103/PhysRevLett.93.261101>
59. Hofmann F, Müller J, Biskupek L. Lunar laser ranging test of the Nordvedt parameter and a possible variation in the gravitational constant. *A&A*. 2010;522, Art. #L5, 3 pages. <http://dx.doi.org/10.1051/0004-6361/201015659>

